

Comparison between computerized tomography and ultrasound systems for treatment planning in RT

Inês Henriques de Carvalho Pino,

Physics Department, Instituto Superior Técnico, Universidade de Lisboa, Lisboa, Portugal

The purpose of this thesis is the comparison of the geometrical uncertainties in image acquisition and planning by the two most commonly used equipments for treatment planning in brachytherapy, computed tomography (CT) and ultrasound (US). The geometrical uncertainties can also be applied on the margins for the clinical target volume (CTV) when one of these image systems is used for setup patients on daily basis in external radiotherapy.

Quality control phantoms were used, such as LAP, CIRS 045A, CIRS 053-MM, Siemens CT phantom, CAPTHAN and also an in-house phantom named as "Ping-Pong". The delineation of structures was also made for both equipments. Finally, estimated dose values in both treatment planning systems were compared to the dose delivered to the phantom.

It was noted that the quality control parameters presented the behavior of a normal distribution, and they were within the tolerances clinically accepted. The data also showed low standard deviation values, which imply the equipments have good reproducibility and have been well maintained and adjusted.

It has been found that manual delineation method from ultrasound images showed a negative volume average, indicating that delineated volumes were in general smaller than the real volumes. This is something to take into account when planning in order to not miss target coverage.

Deviations of 5.10% and -8.16% were obtained between the dose delivered in the treatment and the estimated dose in the treatment planning for CT scans and US images, respectively, indicating that treatment plans using CT images have smaller geometric uncertainties and thus greater precision for brachytherapy.

As a practical example of the results obtained applied to radiotherapy, it was estimated a partial margin for PTV in a case of prostate treatment by external beam radiation therapy and a margin of 2.1 mm should be applied to the CTV in order to produce an adequate PTV.

I. INTRODUCTION

Geometric uncertainties are a constant problem to be addressed in radiotherapy that can make treatment less effective, causing differences between the planned dose and the actually delivered dose. The determination of the Planning Treatment Volume (PTV), which is defined in International Commission on Radiation Units and Measurements (ICRU) issued report nr. 62 (ICRU 62) [1], is then fundamental in order to comprise all existing geometric uncertainties as mechanical stability of machines, structures delineation, internal anatomical movements and patient setup.

Two techniques most often used in radiotherapy are the Computed Tomography (CT scans) and the medical ultrasound systems (US). Both techniques are commonly used in brachytherapy (BT), in order to define the PTV. In spite of having smaller resolution, US does not use ionizing radiation, therefore does not increase the level of dose absorbed by the patient. It is also a very useful method when a quick action is imperative. On the other hand, CT scans have better resolution, allowing a more precise definition of the structures with higher contrast.

In BT sources are directly allocated to the target volume (CTV) defined by the clinician and it is assumed that the geometry is fixed to the target from the planning to the treatment delivery. Thus, the CTV is assumed to be equal to the PTV. Implementation of margins that encompass the existing geometric uncertainties would make sense if it were possible to estimate the error due to: delineation; the imaging techniques used for planning; the actual position of the sources and applicator with the aim of treatment. Since the greater uncertainty fall within the

own process of delineation of structures and for which there is no quality control defined in the literature. Currently, brachytherapy protocols consider $CTV = PTV$, as they fail to take into account the aforementioned uncertainties.

In external beam radiation therapy, one way to achieve smaller margin value in the PTV is the use of daily imaging methods such as US that provide daily information about the structure's location (setup) in a way that complements other techniques such CT scans that have lack of information of that nature [2].

Quality Control (QC) of an equipment is an elementary step in the evaluation and quantification of geometric uncertainties.

This work shows its real importance in the comparison of geometric uncertainties of CT scans and US in the phase of treatment planning, which has no literature reference concerning the area of brachytherapy.

II. METHODS

A CT simulator, Siemens Somatom Sensation Open CT scanner 20-slice, with helical acquisition was used in this work.

The US that was used was a Flex Medicam 400, from BK medical, in B-mode. An intracavitary probe was also used.

For the CT scan tests the following phantoms were used: LAP, CAPTHAN, CIRS 045A, CIRS 053-MM and an in-house phantom called as "ping-pong"; and for US: CIRS 045A, CIRS 053-MM and the "ping-pong" phantom.

The ping-pong phantom was also used to compare the planned dose with different treatment planning techniques. It comprises a ping-pong ball of known volume (volume = 29.06 cm³), three needles with 7 active points each, plastic catheters and a template to guide and hold the needles. Those needles are put inside the catheters and placed through the template with the respective coordinates into the ping-pong ball. Table 1 summarizes all phantoms with respect to each test and Quality Control (QC).

	CT-scan QC	US QC	Delineation test	Comparison of dose test
LAP	X			
CATPHAN	X			
CIRS 045A		X	X	
CIRS 053 MM			X	
Ping-Pong			X	X

Table 1: Phantoms used for each test and QC.

For US acquisition test, the probe is placed inside water, allowing a better propagation of the ultrasounds. Also the planning system for CT scans is done using this setup as the human body is mainly composed by water.

For dosimetry purposes and thus verification of dose to a point in the treatment planning, a MOSFET detector, from Medical Canada (model TN-502RDM-H) is used.

The treatment planning systems were Oncentra Brachy (OB) version 4.5.2 and Oncentra Prostate (OP) version 4.2.21 for CT and US images, respectively.

III. RESULTS

A. Computed Tomography Quality Control

All tests were conducted over two years and were based on the TG 142 [3] from American Association of Physics in Medicine (AAPM). The normality was tested using Shapiro-Wilk test [4]. We found that all parameters followed a Gaussian distribution for a 5% significance level. Paradigmatic examples are: i) the alignment of the left side when facing the gantry (A side) coronal laser; and ii) the image scale in the yy direction.

The data related to the image scale on the Y direction (Fig. 1A) is normally distributed with a significance level of 0.05 ($W=0.989$, $p=0.075 > 0.05$, for a 95% confidence interval). The data relating to the alignment of the coronal A laser (Fig. 1B) follows a normal distribution with a 0.05 significance level ($W=0.994$, $p=0.074 > 0.05$, for a confidence interval of 95%).

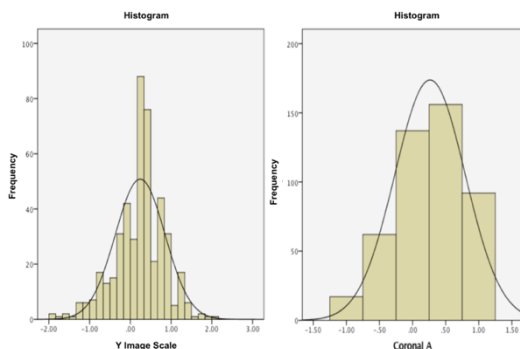


Figure 2: A) Histogram of values relating to the scale test in the Y axis. The black line corresponds to a normal distribution. B) Histogram of values relating to the alignment test of the left laser to the coronal plane.

One of the main tests for Quality Control related to image parameters is the verification of the linear relationship between CT numbers and attenuation coefficients (Fig.2), which is sensitometry test and can be performed by using the CAPTHAN phantom.

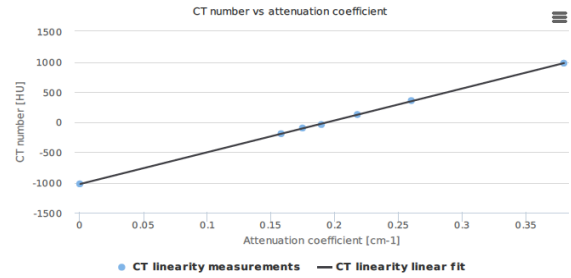


Figure 1: Linear relationship between the CT number (or HU) and the attenuation coefficient of the different materials.

In Table 2 the results obtained for the slice width test using two different methods, spheres/rods and wires, are listed. The results are summarized by the difference between baseline and experimental values, Δ , average, and standard deviation (SD). The negative value indicates that the estimated values of slice width are in average lower than the real width.

	Baseline	Tolerance	Δ average (mm)	SD (mm)
Slice width (wire)	10 mm	± 2 mm	-0.19	0.28
Slice width (spheres)		± 2 mm	-0.21	0.14

Table 2: Results for the slice width test using two different methods.

Slice width with spheres method presents half of the SD compared to the wire method, meaning that the first method is more accurate, giving smaller dispersion of results.

Spatial resolution was also tested for different modulation levels (2%, 5%, 10% and 50%) using the image of a rod (Table 2). It should be noted that the average resolution is about 1/100 of the frequency, except for the modulation at 10% (0.24 cycles/cm).

	Baseline	ToI*	Δ average (cycles/cm)	SD (cycles/cm)	
Spatial resolution (cycles/cm)	MTF 50%	4	10%	-0.06	0.13
	MTF 10%	7	10%	-0.24	0.12
	MTF 5%	7.5	10%	-0.06	0.10
	MTF 2%	8	10%	0.08	0.12

* From hospital baseline

Table 3: Results for the spatial resolution for several MTF values.

In low contrast test, both the average and the standard deviation increases with decreasing contrast between the rods and the background, which means that, the smaller the contrast between two structures (structures with similar HU), the greater is the deviation to the expected value, hindering the distinction of structures with similar HU. There is an inverse relationship between contrast and the size of “details” (Fig. 3) as expected, meaning that for higher contrast (different HU) smaller details (better resolution) can be observed (Table 4).

		Baseline	Tol. [3]	Δ average	SD
Low contrast	Detail 1% contrast	2.0 mm	10%	0.00 mm	0.00 mm
	Detail 0.5% contrast	3.0 mm	10%	0.00 mm	0.00 mm
	Detail 0.3% contrast	4.0 mm	10%	0.00 mm	0.00 mm
Uniformity	Average of HU at the central ROI	16.3 HU	[5-18HU]	-1.61 HU	1.37 HU
	Noise	4.5 HU	± 5 HU	0.17 HU	0.10 HU

Table 4: Results for low contrast and uniformity tests.

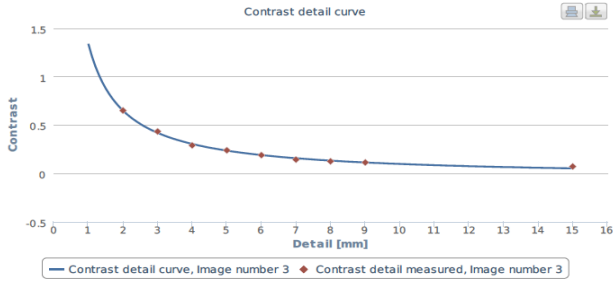


Figure 3: Contrast-detail curve.

B. US Quality Control

One of the phantom used for US QC was the CIRS 045A, which contains three oval structures with different volumes ($V_1=3.5 \text{ cm}^3$, $V_2=8.7 \text{ cm}^3$, $V_3=20.3 \text{ cm}^3$ [5]) and also a group of wires in a "N" configuration at known distances. Tables 5 and 6 show some distance verifications in the axial and sagittal planes. Note that the acquisition in the sagittal plane has a difference of 1 mm in depth in relation to the axial plane. This difference is due the position of the crystals in the probe. Volume determination for these depths is presented in Table 7.

Distances (axial plane)	Baseline (mm)	Δ average (mm)	Difference (%)	SD (mm)
Axial	40	0.05	0.12	0.11
Lateral (proximal)	10	0.06	0.62	0.17
Lateral (distal)	40	0.17	0.41	0.07

Table 5: Values obtained in the determination of the distance between wires, in the axial plane at a depth of 5.7 cm.

Distances (sagittal plane)	Baseline (mm)	Δ average (mm)	Difference (%)	SD (mm)
Axial	10	0.06	0.59	0.07
Lateral (proximal)	5	-0.01	-0.30	0.14
Lateral (distal)	40	0.19	0.48	0.16

Table 6: Values obtained in the determination of the distance between wires, in the sagittal plane at depth of 5.6 cm.

	Baseline (cm^3)	Tolerance (cm^3) [5]	Δ average (cm^3)	Difference (%)	SD (cm^3)
Volume 1	3.6	0.5	0.28	7.91	0.11
Volume 2	8.7	0.5	0.52	5.95	0.17
Volume 3	20.3	0.5	-0.08	-0.39	0.35

Table 7: Determined values for all three volumes at depths of 5.7 cm and 5.6 cm in the axial and sagittal planes, respectively.

These volumes are automatically acquired by the equipment. It appears that there is an increased average value for volume 1 (smaller volume) with a difference of about 8% compared to baseline, whereas the volume 3 (bigger volume) shows a difference of about 0.4% in module.

For smaller volumes, such as volume 1, a small deviation in the delineation conducts to larger differences to the real volume.

Depth - 6.0/5.9 cm					
	Baseline (cm^3)	Tolerance (cm^3) [5]	Δ average (cm^3)	Dif. (%)	SD (cm^3)
Volume 1	3.6	0.5	0.38	10.62	0.18
Volume 2	8.7	0.5	0.45	5.21	0.30
Volume 3	20.3	0.5	0.44	2.16	0.57
Depth - 5.4/5.3 cm					
	Baseline (cm^3)	Tolerance (cm^3) [5]	Δ average (cm^3)	Dif. (%)	SD (cm^3)
Volume 1	3.6	0.5	0.33	9.09	0.16
Volume 2	8.7	0.5	0.48	5.49	0.32
Volume 3	20.3	0.5	0.29	1.44	0.60

Table 8: Volume values for the three structures at different depths. The first depth value corresponds to axial plane and the following value corresponds to sagittal plane.

When assessing different depths, no significant changes in volume were observed (Table 8). Further statistical analysis, revealed that the distributions of the three volumes for all depths (Friedman's test [6]) are statistically similar and may be treated together ($p=0.739 < 0.05$, for a 95% confidence interval).

C. Delineation test in treatment planning systems

Unlike the US technique, where the equipment automatically acquires volumes, in CT is necessary resorting the planning system to assess this parameter.

To study the delineation deviations in the planning procedure using the Oncentra Brachy system, acquisitions were made for the phantoms CIRS 053-MM and CIRS 045A and volumes determined. Table 9 shows the results of the deviations obtained for manual and automatic delineation procedures using CIRS 053-MM and Table 10, CIRS 045A.

Manual delineation with CIRS 053-MM				
Structure	Baseline (cm^3)	Δ average (cm^3)	Dif. (%)	SD (cm^3)
Prostate	~ 53	0.48	0.91	0.48
Automatic delineation with CIRS 053-MM				
Structure	Baseline (cm^3)	Δ average (cm^3)	Dif. (%)	SD (cm^3)
Prostate	~ 53	1.67	3.15	0.35

Table 9: Deviations between manual and automatic delineation of prostate.

The distributions from both methods for delineation of the prostate volume were shown as significantly different, by using the t-test ($p=0.025$ for a 95 % CI). Automatic delineation showed the highest difference to the baseline (3.15%) and the manual delineation showed a difference 0.91%.

Manual delineation with CIRS 045A				
	Baseline (cm ³)	Δ average (cm ³)	Dif. (%)	SD (cm ³)
Volume 1	3.60	0.16	4.43	0.15
Volume 2	8.70	1.10	12.69	0.22
Volume 3	20.3	1.14	5.62	0.16
Automatic delineation with CIRS 045A				
	Baseline (cm ³)	Δ average (cm ³)	Dif. (%)	SD (cm ³)
Volume 1	3.60	0.18	5.00	0.22
Volume 2	8.70	0.95	10.92	0.17
Volume 3	20.3	1.57	7.73	0.19

Table 10: Deviations between manual and automatic delineations for all three oval structures.

In general, differences in volumes are superior for the automatic method, with the exception of volume 2, as showed in Table 10.

The differences obtained between methods used on the CT images can be justified by the fact that the first type of automatic delineation resort to contrast difference between structures and background. Thus the identification of structure boundaries may be hindered in the regions where the image becomes blurred due to transition of media with different absorption coefficients. This limitation depends on the density threshold, influencing the contrast used for displaying the image. The system can identify the structure as being bigger or smaller depending on the level of contrast used. The contrast used for the automatic delineation led to a certain volume value; if another value of contrast is used the volume of the enclosed structure will be different.

However, none of the distributions obtained for the volumes 1, 2 and 3 were significantly different (t-test, $p=0.797$, $p=0.633$, $p=0.615$, respectively). The results indicate that for this phantom the two delineation methods do not differ from each other, showing similar results.

In order to determine volumes manually by US is necessary to resort to the respective planning system as automatic delineation is made directly on the equipment. The automatic delineation referred to 240 measures (3 volumes and 20 times each for 4 different depths) and manual delineation to 20, for ping-pong phantom. The comparison of results between the manual and automatic delineations is found in Table 11.

Manual delineation for US		
	Δ average (cm ³)	SD (cm ³)
Volume	-0.42	1.28
Automatic delineation for US		
	Δ average (cm ³)	SD (cm ³)
Volume	0.11	0.32

Table 11: Results for the manual and automatic delineations with US.

It was found that the manual delineation method has a larger mean (in module) than the automatic delineation method, as expected, since it uses a mathematical algorithm for volumes calculation. Automatic delineation showed much more accuracy than the manual method. Therefore, automatic delineation is significantly more accurate than the manual delineation. This method also has a smaller standard deviation value, indicating that there is less dispersion of obtained volumes compared to the values

obtained with manual delineation. On the other hand, manual delineation shows a negative value of average meaning that smaller volumes than the real ones were obtained.

Statistically, the two distributions were similar ($p=0.414 < 0.05$ for a 95% CI) indicating that there was no significant difference between methods.

To compare the uncertainties estimated of manual delineations by both image systems, CT and US, it was used the ping-pong phantom and the results are summarized in Table 12.

Manual delineation for CT scan		
	Δ average (cm ³)	SD (cm ³)
Volume	0.68	0.22
Manual delineation for US		
	Δ average (cm ³)	SD (cm ³)
Volume	-0.42	1.28

Table 12: Comparison of manual delineation between CT scans and US.

The CT and US distributions were statistically different ($p=0.01$ for a 95% CI), meaning that manual delineation results depend on the equipment.

In fact, the differences in average for the volume based on CT scan images was higher (0.68 cm³) than US (-0.42 cm³). The negative signal indicates that the average volume values are smaller than expected, which means that manual delineation with US gives in general smaller volumes than the real ones, as it was mentioned previously.

However, the standard deviation (associated with random deviation) is lower in manual delineation of CT scan images, indicating less dispersion of the measured values.

In order to compare techniques, it was ensured that the standard error is similar for both equipments. And it depends on the number of tests performed for each device.

Table 13 summarizes the results of the automatic delineations obtained for each technique with a total number of 20 and 240 measurements using CT and US images, respectively.

Automatic delineation for CT scan		
	Δ average (cm ³)	SD (cm ³)
Volume 1	0.18	0.22
Volume 2	0.95	0.17
Volume 3	1.57	0.19
Automatic delineation for US		
	Δ average (cm ³)	SD (cm ³)
Volume 1	0.32	0.15
Volume 2	0.48	0.26
Volume 3	0.21	0.53

Table 13: Comparison of automatic delineation for both imaging techniques.

For larger volume values the average reaches higher values, in the automatic delineation in CT images, whereas in the automatic delineation of US images, for larger volumes, the random deviation becomes larger. This means that in automatic delineation method of CT images, as volumes become larger the deviation from the baseline value becomes greater, while the dispersion values (given by the random deviation) remain relatively constant, which shows that this technique is precise for the range of volumes studied. Furthermore, for automatic delineation in US images, while the deviation value to the baseline

volume value is maintained, the random deviation increases with the volume value, indicating that for greater volumes the dispersion increases. This happens due the fact that bigger volumes reach higher depths where there's an increase dispersion of the ultrasound waves and consequently lower resolution.

When the distributions of volumes 1, 2 and 3 are compared, the significance obtained was $p=0.643$, $p=0.631$, $p=0.047$, respectively, indicating that there is no significant difference (for a 95% CI) between methods for volumes 1 and 2, whereas for volume 3 we cannot conclude anything about its significance.

D. Comparison of dose in treatment planned by the two techniques

The treatment plannings were configured with a source of ^{192}Ir in Oncentra Brachy (for CT scan) and Oncentra Prostate (for US). The conditions of the radioactive source were the same for both planning systems.

The dosimeter was positioned manually, meaning that its location depends directly on the needle/applicator reconstruction which in turn depends on the uncertainty in the determination of the source position and applicator geometry. So, a deviation in determining distances leads to a shift in reconstruction of the needle position and consequently in the determination of the active positions of source or any other points of interest. The coordinates for the position of the dosimeter in treatment (A1) and the respective estimated absorbed dose by the planning system are indicated in Table 14.

Point	X (mm)	Y (mm)	Z (mm)	Absor. Dose (cGy)
A1	-0.2	0.9	1.1	125.74

Table 14: Coordinates for the chosen point as dosimeter location in treatment at the OB system plan and absorbed dose.

This point is marked by an observer in the place where he believes it matches the location of the dosimeter in treatment. A slight deviation from this point reflects a significant change in absorbed dose, as can be inferred from Table 15. It is therefore important to ensure that the location of the point is made accurately, being necessary to be aware of the existing geometric uncertainties.

Point	Y (mm)	Absor. Dose (cGy)
A1	1.0	124.88
	0.9	125.74
	0.8	126.61
	0.2	132.02

Table 15: Absorbed dose planned for each point.

Note that a variation of 0.7 mm from the selected point translates in a difference of 6.28 cGy of absorbed dose (Table 15). As previously stated, the observed point in the planning system incorporates geometric uncertainties from the equipment, and these have to be taken into account into the treatment planning phase. The closer to the radiation source the greater is the variation of dose between points.

Change in dose vs. location related to A1 ($y=0.9$ mm)

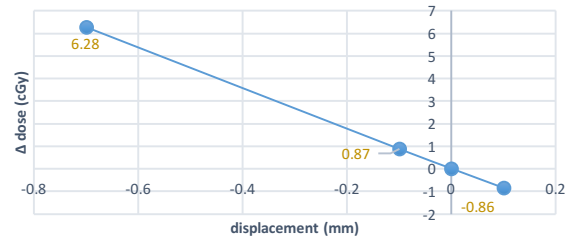


Figure 4: Relationship between displacement position to $y = 0.9$ mm, and difference in absorbed dose.

Resorting to the treatment planning with CT images, the difference between the dose measured during the treatment and the dose planned in the planning system OB (N=4) was approximately 5.10% (Table 16).

Measured dose at treatment by MOSFET	Estimated dose at treatment planning OB (CT)	Dif. (%)
132.5 ± 0.5 cGy	125.74 cGy	5.10

Table 16: Comparison between estimated dose in OB treatment planning system and measured dose in treatment.

Given that the estimated dose has a difference of about 6.76 cGy related to the dose measured at the treatment (Table 16), it means that, by extrapolating the data from Fig.4, the chosen point has about -0.7 mm of displacement in the y direction to the planned location (see Fig.4).

The same procedure described above was used to evaluate the planning system for US.

The chosen point in the planning system dosimeter location (M1) is described in Table 17.

Point	X (mm)	Y (mm)	Z (mm)	Absor. Dose (cGy)
M1	72.23	40.48	11.0	149.10

Table 17: Coordinates for the chosen point as first active point at the OB system plan.

After completing the treatment, it was verified that the estimated value in the treatment planning had a -12.52% deviation for the measured value at the treatment (dose measured = 132.5 ± 0.5 cGy), as shown in Table 18.

Measured dose at treatment by MOSFET	Estimated dose at treatment planning OP (US)	Dif. (%)
132.5 ± 0.5 cGy	149.10 cGy	-12.52

Table 18: Comparison between the estimated dose in OP treatment planning system and measured dose in treatment.

The difference between estimated dose in the planning system and that obtained in the treatment is greater in US, i.e., there is a greater discrepancy between the value predicted by the Oncentra Prostate based on US images and the value measured in the treatment (-12.52%) than the difference between the predicted dose by Oncentra Brachy based on CT images and the value measured in the treatment (5.10 %).

Measured dose at treatment by MOSFET	Estimated dose at treatment planning OB (CT scan)	Dif. (%)	Estimated dose at treatment planning OP (US)	Dif. (%)
132.5 ± 0.5 cGy	125.74 cGy	5.10	149.10 cGy	-12.52

Table 19: Estimated dose for each technique and measured dose during treatment.

The greater discrepancy may mean that the point defined in the Oncentra Prostate planning system is not at the correct location, even if it is taken into account the dosimeter calibration uncertainty of 10% [7]. This may mean that there is greater difficulty in describing points in the planning based on US images than it is in the CT images. So, it was opted to define another point (see Tables 20 and 21). Anyway, the results show the uncertainty inherent of the US images that include user delineation and image distortion.

Point	X (mm)	Y (mm)	Z (mm)	Absor. Dose (cGy)
P1	73.18	39.90	11.20	143.31

Table 20: Coordinates of the new chosen point, P1.

Measured dose at treatment by MOSFET	Estimated dose at treatment planning OB (CT scan)	Dif. (%)	Estimated dose at treatment planning OP (US)	Dif. (%)
132.5 ± 0.5 cGy	125.74 cGy	5.10	143.31 cGy	-8.16

Table 21: Difference of estimated doses in the planning treatment with the new point P1 and measured doses in treatment.

Differing from the geometric location of the selected point in the OB as a dosimeter position in the treatment to the initially selected point, the difference of planned dose and the new chosen point and the treatment dose was determined.

With the new description of the point of measurement, we obtained a difference of -8.16% between planned and treatment doses, thus improving the previous results (12.52%). This means that the displacement performed to the initial point ($\Delta x=0.95$ mm, $\Delta y=0.58$ mm and $\Delta z=0.2$ mm) represents a difference of -3.88% in absorbed dose, showing the importance of geometric precision at the images.

Still, there is a greater difference between planned and treatment values for the US planning system.

Table 21 shows that the uncertainty in determining the geometry of the dosimeter has direct impact on the values of estimated dose in the planning system.

In conclusion, the difference between estimated dose values in the treatment planning and the values measured during treatment (actual values) is smaller for treatment planning with CT images, which means that these plans are carried out more accurately by showing smaller geometric deviations. Therefore, the error in source position leads to significant differences of dose between techniques.

Given that the treatment is the same for both plans, then the location of the selected point of measurement is the

only variable, which means that the location determined in the plan based on CT images is closest to the actual geometry, reflecting the value of planning with CT upon US where it was found the greater geometric uncertainty.

Therefore, when using a plan based on US images, one must have careful attention in the definition of the needles and the positions where the sources will be positioned as the definition in the image is not as accurate as in CT scans, those plans have higher geometric uncertainty. This difference may be explained by several factors: resolution of the imaging system can cause geometric deviations in position/distance of the object and also there's a 1mm discrepancy in depth of sagittal and axial planes due to the crystals position in the probe.

E. Geometric uncertainties in radiotherapy

To study geometric uncertainties associated to each technique, it's necessary to know what's the clinical objective as there are specific parameters that only exist depending on the use of the equipment. For example, CT scans are used in both types of radiotherapy (brachytherapy and external beam radiation therapy), but the use of lasers only happens in external beam radiation therapy, which means that in this case it is necessary to take into account this "new" source of deviation. On the other hand, one must know how to evaluate the type of uncertainty (systematic or random) and its origin (internal/anatomical movements or external/setup).

In this paper, only geometric uncertainties resulting from the image equipment to the planning phase (distance calculation, automatic determinations of volumes and manual delineation of volumes in the planning system) were studied.

1) Brachytherapy

For this type of radiotherapy, we may use images from CT scans or US for treatment planning.

For CT scans there are three types of geometrical uncertainties, while determining: object geometry and source position; volumes and their uncertainties defined manually or automatically in the planning systems. The results for source positions deviations in the three directions are presented in Table 22.

		Δ average (mm)	Dif. (%)	SD (mm)
Distance	X	-0.25	0.17	0.73
	Y	0.24	0.18	0.61
	Z	0.32	0.82	0.45

Table 22: Source position uncertainties for the three directions.

From Table 22 it can be seen that the systematic error component of the source position in the x direction has a negative value, meaning that there is a displacement of the Gaussian to the left. This indicates that the measured values are generally shifted laterally to the needle. In the y direction, it is found that the shift was toward the needle extremity.

Ideally, the average would be zero, meaning that the measured value would be exactly equal to the value of the object position. In this case, the fact that a deviation in point position means that the calculated distance between two points do not actually correspond to the actual distance. In practice, if the distance between the needle tip

and the template in the ping-pong phantom is determined in the planning system based on CT images (OB), two cases may occur: i) if the systematic error is positive, the estimated distance is greater than the actual distance, ii) if the systematic error is negative, the estimated distance is less than the actual distance.

The systematic (Σ) and random (σ) components of the distance uncertainty ($e_{distance}$) respectively, the following equations were used:

$$\Sigma_{distance} = \sqrt{\Sigma_x^2 + \Sigma_y^2 + \Sigma_z^2} \quad (1)$$

$$\sigma_{distance} = \sqrt{\sigma_x^2 + \sigma_y^2 + \sigma_z^2} \quad (2)$$

An $e_{distance} = 0.47 \pm 1.05$ mm was obtained. Thus, all calculated distances using reconstructed images from CT scans will have this associated error.

Volume and delineation deviations (and consequently the calculation of PTV) were studied using the phantoms CIRS 045A and CIRS 053-MM. Table 23 shows the results for all geometric uncertainties in images based on CT scans.

	Σ (systematic error)	σ (random error)
Distance (mm)	0.47	1.05
Volume (cm ³)	1.22	0.21
Delineation (cm ³)	0.68	0.22

Table 23: Summary of systematic and random components of distance, volume (automatic delineation) and (manual) delineation errors for CT scan.

In US, there are again three types of geometric uncertainties: object geometry and source position; volumes and their uncertainties defined manually in the planning systems or automatically with the probe and the US system. Table 24 shows the results for distance uncertainties measured in sagittal and axial planes.

Axial plane

Distance	Σ (systematic error)	σ (random error)
Axial (mm)	0.02	0.11
Average Lat. Proximal (mm)	0.08	0.16
Total (mm)	0.09	0.20

Sagittal plane

Distance	Σ (systematic error)	σ (random error)
Axial (mm)	0.03	0.08
Average Lat. Proximal (mm)	0.04	0.13
Total (mm)	0.05	0.16

Table 24: Errors in distance determination for acquisitions in axial and sagittal planes. Total error comes from the combination of axial and lateral components.

In order to determine volume deviations in the planning system (OP), a set of manual delineations of the ping-pong ball (which has a known volume) was made. The resulting error was $e_{volume} = 0.11 \pm 0.32$ cm³.

The delineation error in the US was determined by making the automatic calculation of the three existing oval structures in the CIRS 045A and the respective deviations

from the value given by the manufacturer. The total error includes the three different volumes, which provide more information about the existing deviations. Table 25 summarizes the results of the US and CT systems for brachytherapy.

US		
	Σ (systematic error)	σ (random error)
Dist. axial plane (mm)	0.09	0.20
Dist. sagittal plane (mm)	0.05	0.16
Volume (cm ³)	0.11	0.32
Delineation (cm ³)	-0.42	1.28
CT scan		
	Σ (systematic error)	σ (random error)
Distance (mm)	0.47	1.05
Volume (cm ³)	1.22	0.21
Delineation (cm ³)	0.68	0.22

Table 25: Comparison between final uncertainties from the two systems.

Although the systematic error of the distance in each individual plane was smaller for US, the location of a point in space corresponds to its three coordinates, that is, in the two planes simultaneously. As mentioned above, there is a discrepancy of 1 mm between planes at which the total error of distance becomes higher for US, as can be seen in the planning system.

The systematic error in determining the volume, as discussed above, is smaller for US because the analyzed structures have regular form and the algorithm resort to mathematical equation of volumes, although this does not happen in the clinical routine. However, the random deviation is also higher for US.

Using manual delineation, the CT-scans is the most accurate technique (with smaller random deviation).

2) External beam radiation therapy

In external radiation therapy only the first two stages of the process, image acquisition for treatment planning and delineation of the structures, were considered, as previously mentioned. The geometric uncertainties obtained using CT images are summarized in Table 26.

	Σ (systematic error)	σ (random error)
Lasers (mm)	0.27	0.42
Image reference plane (mm)	0.18	0.30
Distance (mm)	0.47	1.05
Autom. delineation (cm ³)	1.22	0.21
Manual delineation (cm ³)	0.68	0.22

Table 26: Geometric uncertainties from several sources to be taken into account when using CT scans for external beam radiation therapy purposes.

A case study of a prostatic patient subjected to external radiation was examined to illustrate how these uncertainties are taken into account for the definition of PTV, considering that imaging was performed daily.

	Σ (systematic error)	σ (random error)
Prostate mov. [8] (mm)	0.4	0.7

Table 27: Specific information for this illustrative example about prostatic treatment.

In order to determine the margin for the clinical volume (CTV) we used the model given by Stroom *et al.* [9] that ensures that at least 99% of the CTV receives at least 95% of prescribed dose. The model of Stroom gives an expression for the margin to add to the CTV that incorporates all geometric uncertainties and it's given by the following expression:

$$\text{Margin} = 2\Sigma_{total} + 0.7\sigma_{total} \quad (3)$$

The total systematic error Σ_{total} and the total random error σ_{total} are given as follows [8]:

$$\Sigma_{total} = \sqrt{\Sigma_{deli}^2 + \Sigma_{in}^2 + \Sigma_{ext}^2} \quad (4)$$

$$\sigma_{total} = \sqrt{\sigma_{deli}^2 + \sigma_{int}^2 + \sigma_{ext}^2} \quad (5)$$

The following factors were considered as uncertainties (Table 26): all distances measurements using lasers, the coincidence between the reference plane and the imaging plane, automatic delineation and prostatic motion during treatment. In this exercise, the uncertainties associated with the positioning of the patient in the treatment equipment and those associated with the treatment equipment were not considered, as this was beyond the scope of the work. Therefore, $\Sigma_{ext} = 0$. For this reason, the margin to the CTV calculated in this exercise is denominated as partial PTV.

Considering that the automatic delineation uncertainty was obtained volumetrically, one has to proceed to the volume derivation to obtain the radial variation of volume, in order to add to the equations 4 and 5. As the volume was a sphere (ping-pong ball), the process of derivation is straightforward. The partial margin obtained considering the conditions described was 2.1 mm.

F. Conclusion

The study in this paper provides for clinical routine perception, in a quantitatively way, the impact that different imaging methods have in the planning process for radiotherapy, especially with respect to brachytherapy where it is considered that the volume clinically defined is equal to the planning treatment volume and therefore are not considered geometric uncertainties associated to the planning and treatment phases. It showed the importance of the implementation of quality control for the delineation phase and the impact of uncertainties related to the planning phase (pre-setup patient equipment) in the volume for treatment.

The comparison between two imaging methods as carried out in this work provided a quantitative assessment of uncertainties in CT and US images applied to radiation therapy. This is of the utmost importance to improve the

perception of the impact of different imaging methods in radiotherapy treatment planning.

Although both imaging QC processes showed results within the clinically accepted tolerances, when a comparison between techniques is made, it is possible to know the impact of geometric uncertainties associated with each of them in the planning.

CT scan is presented as the most accurate method compared to US for both BT and external beam therapy.

Although US is not an imaging method as accurate as CT, it is very useful for ERT as a method of daily image that does not use ionizing radiation and allows the reduction of setup errors [10]. For BT, US allows that treatment planning is carried out more quickly, avoiding dose changes due to variations in the prostatic volume between planning and treatment delivery.

This work enabled the estimation of geometric uncertainties related to the reconstruction of the applicator and in the determination of the positions of the source at inside the phantom, as well as the impact of geometric uncertainties associated with automatic and manual delineations in both planning systems (with CT-scan and US) (Tables 12 and 13). It was also studied the impact of the differences between estimated dose by the planning systems of each imaging equipment due to the uncertainty in determining the position of the dosimeter and the dose effectively delivered. The results showed that brachytherapy planning based on CT images has lower geometric uncertainties compared to US based plans.

Finally, a methodological implementation of the uncertainties obtained in the first stage of the treatment process (planning phase) for estimating margins of target volumes in external beam radiotherapy was applied to a case study.

The systematic error regarding delineation with US showed a negative value, meaning that the planned target volume is sub-estimated, which may lead to a loss in tumor control. These results call the attention for the importance of recognizing the impact of uncertainties in US planning.

However, there are still many topics to be further addressed and investigated, such as: optimization of the image quality parameters in order to improve image quality for radiotherapy purposes, maintaining the correlation HU and electron density to be used in the treatment planning system; study of the use and limitations of the extended field of view (eFOV) for patients with large dimensions, which can cause distortions in the image; optimization of CT-simulator image quality and artifact detection especially in patients with prosthesis. Furthermore, a study of the image QC for a planar probe in patients with breast tumors, should also be part of future work.

G. References

- [1] International Commission on Radiation Units and Measurements, "ICRU Report 62. Prescribing, Recording, and Reporting Photon Beam Therapy (Supplement to ICRU Report 50)," *J. ICRU*, no. November, p. Ix +52, 1999.
- [2] J. C. Ye, M. M. Qureshi, P. Clancy, L. N. Dise, J. Willins, and A. E. Hirsch, "Daily patient setup error in prostate image guided radiation therapy with fiducial-based kilovoltage onboard imaging

and conebeam computed tomography.,” *Quant. Imaging Med. Surg.*, vol. 5, no. 5, pp. 665–72, 2015.

- [3] E. E. Klein, J. Hanley, J. Bayouth, F. F. Yin, W. Simon, S. Dresser, C. Serago, F. Aguirre, L. Ma, B. Arjomandy, C. Liu, C. Sandin, T. Holmes, and A. A. of P. in M. Task Group, “Task Group 142 report: quality assurance of medical accelerators,” *Med Phys*, vol. 36, no. 9, pp. 4197–4212, 2009.
- [4] S. S. Shapiro and M. B. Wilk, “An Analysis of Variance Test for Normality (Complete Samples),” *Biometrika*, vol. 52, no. 3–4, pp. 591–611, 1965.
- [5] U. P. Phantom, “Brachytherapy QA Phantom 045,” no. 800, pp. 131–132.
- [6] M. R. Sheldon, M. J. Fillyaw, and W. D. Thompson, “The use and interpretation of the Friedman test in the analysis of ordinal-scale data in repeated measures designs,” *Physiother. Res. Int.*, vol. 1, no. 4, pp. 221–228, 1996.
- [7] T. N. R. Ribeiro, “Estudo e implementação de dosimetria com mosfet em braquiterapia de alta taxa de dose,” p. 76, 2010.
- [8] A. J. Nederveen, U. A. van der Heide, H. Dehnad, R. J. van Moorselaar, P. Hofman, and J. J. W. Legendijk, “Measurements and clinical consequences of prostate motion during a radiotherapy fraction,” *Int. J. Radiat. Oncol. Biol. Phys.*, vol. 53, no. 1, pp. 206–214, 2002.
- [9] J. C. Stroom and B. J. M. Heijmen, “Geometrical uncertainties, radiotherapy planning margins, and the ICRU-62 report,” *Radiother. Oncol.*, vol. 64, no. 1, pp. 75–83, 2002.
- [10] M. E. R. Poli, W. Parker, H. Patrocinio, L. Souhami, G. Shenouda, L. L. Campos, and E. B. Podgorsak, “An Assessment of PTV Margin Definitions for Patients Undergoing Conformal 3D External Beam Radiation Therapy for Prostate Cancer Based on an Analysis of 10,327 Pretreatment Daily Ultrasound Localizations,” *Int. J. Radiat. Oncol. Biol. Phys.*, vol. 67, no. 5, pp. 1430–1437, 2007.